

A MICROGRIPPER WITH A RATCHET SELF-LOCKING MECHANISM

Y.C. Hao, W.Z. Yuan, H.M. Zhang and H.L. Chang
Northwestern Polytechnical University - MEMS Lab, Xi'an, China

ABSTRACT

This paper reports a new design for an electrostatic actuated microgripper with a ratchet self-locking mechanism. The self-locking mechanism enables long-time gripping without continuously applying the external driving signal, such as an electrical, thermal or magnetic field, which significantly reduces the effect and damage on the gripped micro-scale objects that are induced by the external driving signals. The microgripper is fabricated using a silicon-on-insulator (SOI) wafer with a 30 μm device layer. The jaw gap is 100 μm , and the ratchet locking interval is 10 μm . A metal wire is successfully gripped to demonstrate the feasibility of the ratchet self-locking mechanism.

INTRODUCTION

Microgrippers with inherent advantages in operating micro-scale objects have found important applications in micro-assembly and biological research. Numerous microgrippers with different actuating mechanisms, such as electrostatic[1], thermal[2], piezoelectric[3], magnetic[4], pneumatic[5], and direct mechanical contact approaches[6], have been reported in recent decades. However, the existing microgrippers may encounter problems in manipulating micro-devices and biological tissue in the experiments that last for hours or longer. The electrostatic, thermal, piezoelectric and magnetic actuating mechanism may affect or even damage the micro-devices and biological tissues with its electrical, thermal and magnetic power. Accurately controlling the small movement on a micron scale is difficult using the pneumatic and direct mechanical contact method.

In this paper, we introduced a ratchet self-locking mechanism into our existing microgripper[7] to reduce the damage caused by the additional electrical, thermal or magnetic fields. The ratchet mechanism is a one-way intermittent motion mechanism and has been successfully used in micro electro mechanical systems (MEMS) actuators[8] as a locking mechanism. However, the ratchet pawl in [8] is a passive mechanism and cannot separate from the ratchet tooth by control. In our design, the ratchet pawl can separate from the ratchet tooth when an electrostatic actuator is used to release the objects. The designed ratchet self-locking mechanism that enables the microgripper only requires a driving signal in the moment of gripping and releasing the objects, which significantly reduces the duration of exposure of the objects to electrical, thermal or magnetic fields, and it is particularly remarkable in long-time experiments.

DESIGN

The operating principle of the ratchet self-locking mechanism is schematically shown in Figure 1: (a) original state of the ratchet self-locking mechanism; (b) rotation or movement of the ratchet tooth forces the ratchet pawl to move upward; (c) when it crosses the tip of the ratchet

tooth, the ratchet pawl engages with the ratchet tooth and inhibits the inverse of the ratchet mechanism; and (d) when the ratchet pawl and ratchet tooth are separated by an external force, the ratchet mechanism is free and can return to the initial position. Thus, the ratchet self-locking mechanism can lock the microgripper when objects are manipulated without a driving signal.

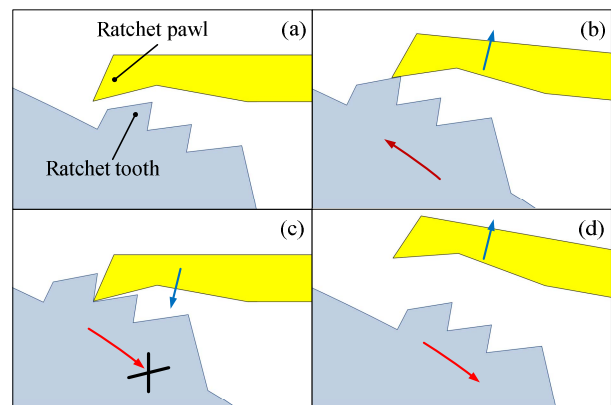


Figure 1: Operating principle of the ratchet self-locking mechanism.

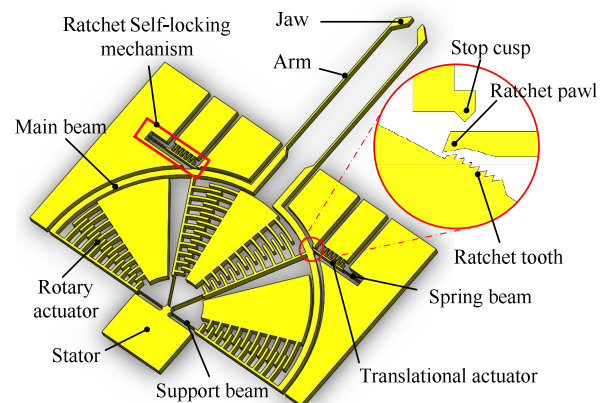


Figure 2: Schematic view of the microgripper.

As shown in Figure 2, the designed microgripper consists of an anchor that fixes the entire microgripper on the substrate; support beams that suspend the remainder of the microgripper and supply the elastic deformation, which is caused by the rotary actuator that drives the main beam; the main beams and the arms, which transfer and amplify the displacement; jaws that directly contact the targets; and the ratchet self-locking mechanism, which restricts the opening of the jaws and dominates the release of the target. In detail, the ratchet self-locking mechanism consists of multiple parts: spring beam, translational actuator, ratchet pawl, ratchet tooth and stop cusp. The engagement of the ratchet pawl and ratchet tooth prevents the jaws from inverse movement and locks the targets, and the translational actuator can set the targets free by separating the ratchet pawl and ratchet tooth. The stop cusp is

designed to prevent the pulling-in of the translational actuator.

The intermittent displacement of jaws is determined based on the size of the ratchet pawl and ratchet tooth, which is confined using the MEMS fabrication process. Considering the mentioned confine, the geometric structure is optimized. As shown in Figure 3, the ratchet teeth are designed to be 3 μm tall and 4 μm wide. The angle of the pawl is 5 degree smaller than the tooth root angle of 60° to easily engage and separate. The tip of the ratchet pawl is on the root circle of the ratchet teeth, and the root circle coincides with the rotation center of the microgripper. The angle between the tip of the ratchet pawl and the root of the first ratchet tooth is 0.4°, and the angle for each tooth is 0.2°. For the designed microgripper, the jaws are closed with a 50 μm movement when the main beam rotates 1°. Thus, the first engagement occurs when the jaw moves 20 μm , but subsequent engagement occurs when the jaw moves 10 μm . The engagement and separation occur when the jaw reaches a displacement of 20 μm , 30 μm , 40 μm and 50 μm . The space between the jaws ranges from 0 to 100 μm , so the microgripper can grip a target with a size of 20 μm , 40 μm and 60 μm . Considering the elastic deformation of the slender arms, the designed microgripper can also grip objects that are slightly larger than 20 μm , 40 μm and 60 μm .

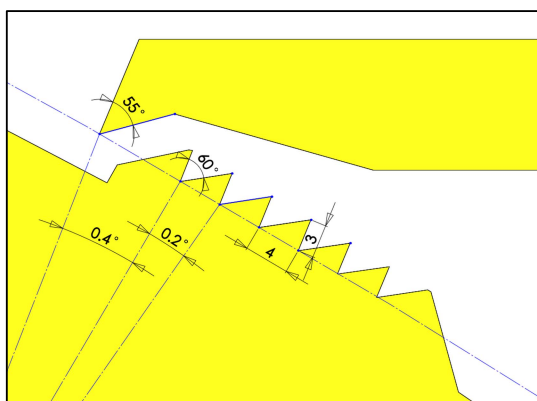


Figure 3: Detailed geometrical specification of the ratchet pawl and ratchet tooth.

FABRICATION

The microgripper is fabricated on an SOI wafer. The SOI wafer has a 400 μm thick substrate, 4 μm thick SiO_2 and 30 μm thick device layer. The fabrication process flow is shown in Figure 4.

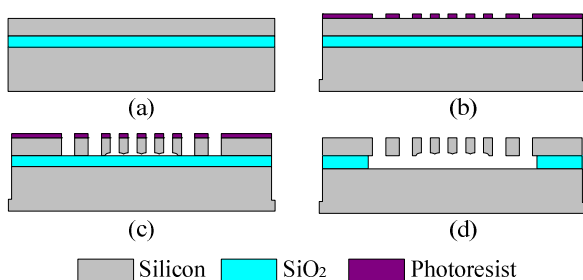


Figure 4: Microgripper fabrication process based on an SOI wafer.

In step (a), the SOI wafer is cleaned with a hydrofluoric acid solution to enhance the adhesiveness of the photoresist; step (b) is patterning by photo resist and dicing but reserving 150 μm ; step (c) is a high-aspect-ratio deep reactive ion etching (DRIE) process with several minutes over etching; and step (d) removes the photoresist and is the wet-release step. The fabricated microgripper can freely move after the releasing by the hydrochloric acid solution. Then, the chip is split, and the fabrication is completed.

A scanning electron microscope (SEM) image of the fabricated microgripper is shown in Figure 5: (a) shows the global view of the fabricated microgripper, and the general size is 3,000 x 4,000 μm ; (b) is the local view of the ratchet mechanism and shows the morphology of the ratchet tooth and ratchet pawl; and (c) shows the jaws, and the space between the jaws is 100 μm .

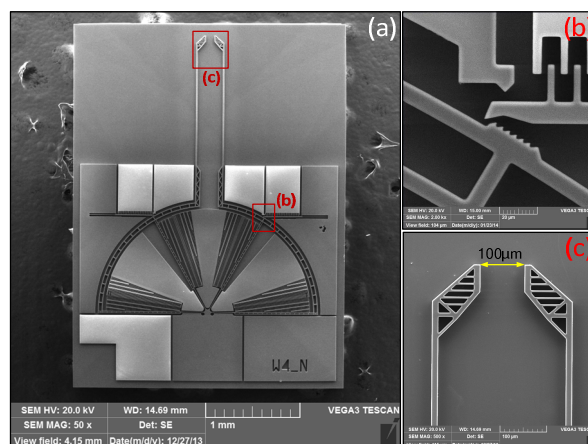


Figure 5: SEM of the fabricated microgripper.

EXPERIMENTAL SETUP AND RESULTS

A peripheral control and observing system is necessary to operate the microgripper. As shown in Figure 6, the control and observing system consists of a printed circuit board (PCB) as the microgripper carrier, a position platform with three degrees of freedom (3-DOF) to control the microgripper position, a transport probe to inject samples, a voltage source to supply the driving voltage, a high voltage amplifier to increase the driving signal, and a microscope for observing.

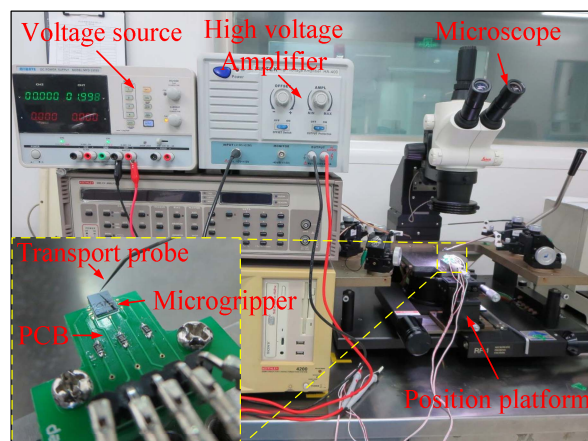


Figure 6: Apparatus setup and arrangement.

Without gripped targets, the voltage is recorded every time the ratchet pawl engages or separates with a ratchet tooth. As presented in Figure 7, the red dots are the measured value of the driving voltage when engagement occurs, and the black line is the analytical relationship between the voltage and the displacement. The dotted line is the fitting curve of the measured value of the driving voltage. Table 1 shows the measured voltage that separates the ratchet tooth and ratchet pawl for different position of the jaws. The deviation between the analytical value and the measured results mainly comes from the approximation in the formula derivation, machining error in the MEMS fabrication and, particularly, the effect of adhesion and friction, which is caused by the contact of the ratchet tooth and ratchet pawl.

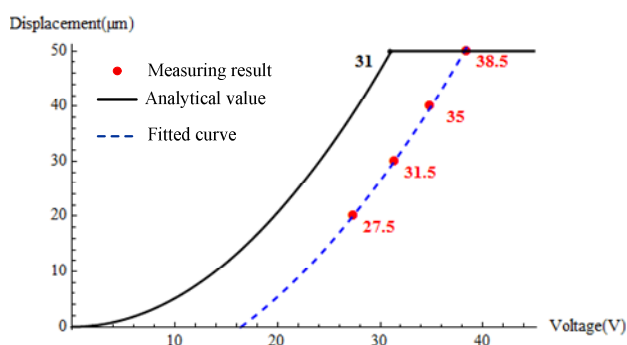


Figure 7: Relationship between the driving voltage and displacement of the jaw.

Table 1: Voltage to separate the ratchet tooth and ratchet pawl.

Displacement of jaw (μm)	20	30	40	50	Analytical value
Separation voltage (V)	58.5	65	70.5	76	22

The performance of the designed microgripper is assessed by gripping a metal wire with a diameter of 1.6 mil ($40.64 \mu\text{m}$). The experiment is shown in Figure 8: (a) positioning the microgripper and preparing to handle the metal wire; (b) the rotary actuator is applied with a driving voltage of 35.5 V to grip the metal wire; and (c) the metal wire is released with a voltage of 77 V on the translational actuator.

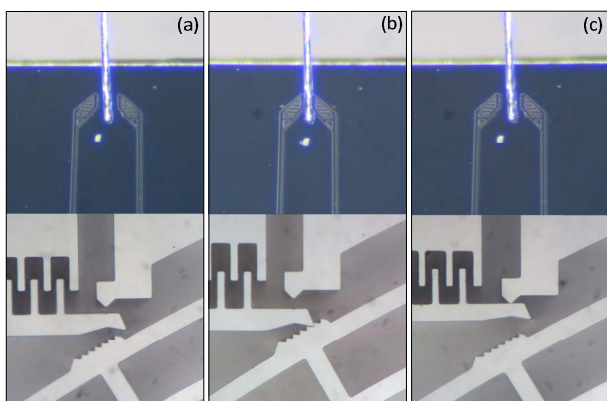


Figure 8: Experimental demonstration of gripping.

The diameter of the metal wire is $0.64 \mu\text{m}$ larger than $40 \mu\text{m}$, and the actuator must overcome the elastic force produced by the arm deformation to lock and release the metal wire. Thus, the voltage applied on the rotary actuator and the translational actuator is larger than the corresponding value in Figure 7 and Table 1. Hence, the deformation of the slender arm can tolerate the size deviation to some extent and make the microgripper more practicable and flexible.

CONCLUSION

An electrostatic microgripper with a ratchet self-locking mechanism is presented. The feasibility of the microgripper has been successfully demonstrated by gripping a metal wire. Currently, the microgripper can handle targets with a size of approximately $20 \mu\text{m}$, $40 \mu\text{m}$ and $60 \mu\text{m}$, but the range can be expanded to several microns or hundreds of microns according to the requirement by adjusting the position of the ratchet tooth and the space of the jaws.

ACKNOWLEDGMENTS

This work was supported by the Chinese National Science Foundation (Grant no 61273052); in part by the Fundamental Research Funds for the Central Universities (Grant no 3102014JC02010505) and 111 project (Grant no B13044).

REFERENCES

- [1] C.-J. Kim, A. P. Pisano, R. S. Muller, and M. G. Lim, "Polysilicon microgripper," IEEE 4th Tech. Dig. Solid-State Sens. Actuator Work., 1990.
- [2] K. Kim, X. Liu, Y. Zhang, and Y. Sun, "Nanonewton force-controlled manipulation of biological cells using a monolithic MEMS microgripper with two-axis force feedback," J. Micromechanics Microengineering, vol. 18, no. 5, p. 055013, May 2008.
- [3] D. H. Wang, Q. Yang, and H. M. Dong, "A Monolithic Compliant Piezoelectric-Driven Microgripper: Design, Modeling, and Testing," IEEE/ASME Trans. Mechatronics, vol. 18, no. 1, pp. 138–147, Feb. 2013.
- [4] T. Ger, H. Huang, W. Chen, and M. Lai, "Magnetically-controllable zigzag structures as cell microgripper," Lab Chip, vol. 13, no. 12, pp. 2364–9, Jun. 2013.
- [5] A. Alogla, P. Scanlan, W. M. Shu, and R. L. Reuben, "A scalable syringe-actuated microgripper for biological manipulation," Sensors Actuators A Phys., vol. 202, pp. 135–139, Nov. 2013.
- [6] B. A. Wester, S. Rajaraman, J. D. Ross, M. C. Laplaca, and M. G. Allen, "Development and characterization of a packaged mechanically actuated microtweezer system," Sensors Actuators A Phys., vol. 167, no. 2, pp. 502–511, Jun. 2011.
- [7] H. Chang, H. Zhao, J. Xie, Y. Hao, F. Zhang, and W. Yuan, "Design and fabrication of a rotary comb-actuated microgripper with high driving efficiency," in 2012 IEEE 25th International Conference on Micro Electro Mechanical Systems (MEMS), 2012, no. February, pp. 1145–1148.
- [8] S. Barnes, S. Miller, M. Rodgers, and F. Bitsie,

“Torsional ratcheting actuating system,” in 2000 International Conference on Modeling and Simulation of Microsystems - MSM 2000, 2000, no. 505, pp. 273–276.

CONTACT

*Honglong Chang, tel: +86-029-8849-2841;
changhl@nwpu.edu.cn